Sensor-Based Contact Geometry Optimization for Multifingered Robot Hands *

Roderic A. Grupen and Jefferson A. Coelho Jr.

Laboratory for Perceptual Robotics
Department of Computer Science
University of Massachusetts, Amherst

Abstract

This paper employs a behavior-based approach to regulate the contact geometry during a dextrous (fingertip) grasp. The goal is to provide a framework for sensor-based controllers that acquire information on-line and use this data stream to refine grasp solutions. We will present two such behaviors and illustrates how they can be used to suppress local errors in the neighborhood of a grasp solution. We present a class of objects for which our behavioral repertoire is globally competent for 2, 3, and 4 contacts, and report the performance of the grasp regulator on this class of objects. This work is part of a larger treatment for a 20 degree of freedom (DOF) eye/hand/arm system under development at the Laboratory for Perceptual Robotics.

Introduction

Success in dextrous manipulation tasks, as in any other real-time task involving interaction with the environment, implies considering perception and action as integral parts of the controller. Integrating perception and action in dextrous hands requires answers to a number of independently challenging questions. Among these: how can dimensionality be used to advantage, what type of information is relevant and what representation should this knowledge employ, how should such a system express manipulation goals, and how can model uncertainty be accommodated by monitoring sensor data during the execution of a grasp.

The complexity of robot path planning is exponential in the number of degrees of freedom (DOF) of the system. Moreover, complete process models are required. Acquiring and maintaining complete models can be as expensive as combinatoric path optimization. The solution usually adopted to both problems is (1) to decompose the complex state space into tractable subspaces, each one controlled by a different *behavior*, and (2) to direct sensory resources to important features of the control process.

*This work is supported in part by NSF CDA-8922572 (CII), IRI-9116297, IRI-9208920 (CRICCS), and CNPq 202107/90.6

Related Work

Considerable progress in grasp planning has been published in the 1980's. The Grip Transform was developed to express the transformation from a set of contact forces or velocities to a net object frame force or velocity[9, 13]. Mathematical programming techniques employing frictional constraints have been described to formulate the grasp force solution[5, 8, 10].

The problem of designing the grasp configuration has also received a good deal of attention. Results have been reported for several "knowledge-based" grasp planners. Fast geometric algorithms for finding force closure contact geometries for polygonal (planar) objects have developed [11] and have been extended (to significantly slower algorithms) for two contacts on piecewise polynomial planar objects[4]. Other work derives grasp controllers from human grasp taxonomies[3]. We refer to this perspective as "knowledge-based" because they rely to a large degree on complete geometric information about the world in the first case, and because they rely on emulating human grasps in the latter case. Grasping has also been approached as an optimization problem. Jameson and Leifer describe a system which optimizes a grasp goal function[7]. Artificial potential fields which avoid first order slip conditions and which penalize unfavorable contact geometries are superimposed to generate a search space. These potential fields penalize contacts near the tip of the finger, the palm, contacts near the table top, and finger configurations with extreme joint angles. This work also requires complete geometry.

Complexity and dimensionality issues have led to behavior-based system architectures. In this paradigm, complex state spaces are decomposed into tractable subspaces which form a basis for all system behaviors [1, 12]. This *factorization* greatly enhances run-time performance. For example, the subsumption architecture[2] and Raibert's hopping platforms[12] partition a complex state space into disjoint controllers that are activated by sensory events. It has been demonstrated that this approach can be used to generate controllers for rather complex processes.

The "Grasp" Problem

The control goal for our system is in general a convex set of wrenches (or generalized forces) that we wish to transmit from the robot manipulator to the object through point contacts. A particularly important class of such tasks is the construction of a stable grasp. We have formulated a sufficiency metric as the basis for optimizing the contact geometry with respect to grasp stability. The contact geometry is *sufficient* if the contact forces are linearly dependent, that is, any contact wrench can be generated by an equivalent linear combination of other contact wrenches in the grasp.

The sufficiency metric is expressed as a quadratic form on the residual wrench vector, $\vec{\rho}$,

$$\begin{aligned} \epsilon_S &= \vec{\rho}^T \vec{\rho} \\ &= \left(\vec{t} - \frac{1}{n}\sum_{i=1}^{n} \hat{\omega}_i\right)^T \left(\vec{t} - \frac{1}{n}\sum_{i=1}^{n} \hat{\omega}_i\right), \quad (1) \end{aligned}$$

where $\vec{\rho}$ expresses the net wrench over $1 \leq j \leq n$ contacts, $\vec{t}$ is an optional wrench closure *bias*, and $\vec{\omega}_i$ is the wrench vector resulting from the i^{th} interaction force. The elements, $t_j \in [-1, 1]$, of $\vec{t}$ and the elements, $w_{ij} \in [-1, 1]$ of $\vec{w}_i$ are qualitative in the sense that they do not reflect engineering units of force and torque, but express the relative ability of a contact configuration to transmit forces and torques through the object's surface. The solution contact geometry is an optimization based on shape rather than dimension.

The wrench vector $\vec{\omega}_i$ can be expressed in terms θ_i, the contact angle for contact i. Differentiating Equation 1 with respect to θ_i yields:

$$\begin{aligned} \frac{\partial \epsilon_S}{\partial \theta_i} &= 2\left(\vec{t} - \frac{1}{n}\sum_i \hat{\omega}_i\right)^T \frac{\partial\left(\vec{t} - \frac{1}{n}\sum_i \hat{\omega}_i\right)}{\partial \theta_i} \\ &= -2\left(\vec{t} - \frac{1}{n}\sum_i \hat{\omega}_i\right)^T \frac{\partial \omega_i}{\partial \theta_i}\frac{1}{n} \\ &= -\frac{2}{n}\vec{\rho}^T G_i \\ &= -\frac{2}{n} G_i^T \vec{\rho}, \quad (2) \end{aligned}$$

and, therefore,

$$\begin{aligned} \frac{\partial \epsilon_S}{\partial \vec{\theta}} &= -\frac{2}{n}\begin{bmatrix} G_1^T \\ G_2^T \\ \vdots \\ G_n^T \end{bmatrix} \vec{\rho} \\ &= -\frac{2}{n} G^T \vec{\rho}. \quad (3) \end{aligned}$$

Equation 3 evaluates to $\vec{0}$ in one of two conditions: (a) $\vec{\rho} = \vec{0}$ and (b) when $\vec{\rho}$ is orthogonal to G^T such that $G^T \vec{\rho} = \vec{0}$. The first condition is the desired convergence criterion and results in a grasp geometry that can be *scaled* to span the task. The second condition is equivalent to a local minimum of ϵ_S. This class of minima results when a local tangent to the wrench surface, G, is orthogonal to the residual vector, $\vec{\rho}$.

Figure 1(a) demonstrates these two types of equilibrium grasp configurations. This figure illustrates the wrench functions, $f_x(\theta)$, $f_y(\theta)$, and $m_z(\theta)$, the error surface ϵ_S, and the positions of attractors in the metric space for a square shape. In this figure, a contact is located at $\theta = 0$ (solid circle) and the error surface is used to regulate the position of the second contact.

Both contacts are modeled as frictionless point contacts. The moving contact will migrate toward one of four separate attractors in the error metric depending on the initial configuration. Of these equilibrium grasp configurations, only the global minimum is a

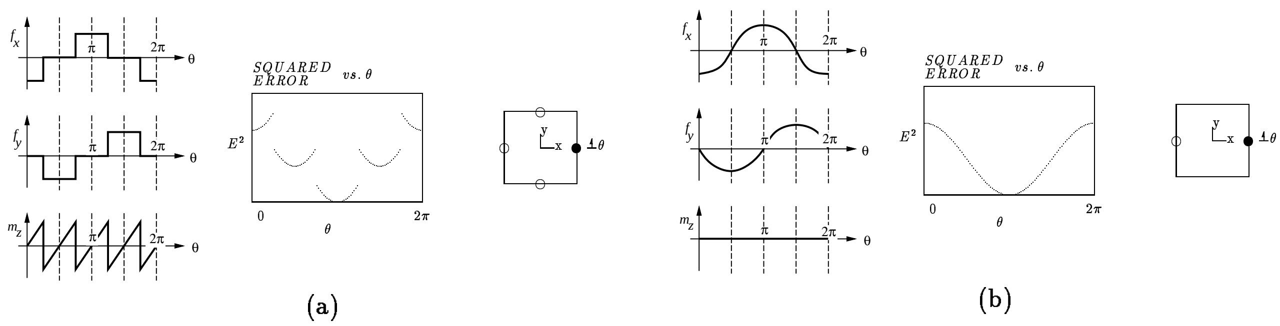

Figure 1: The wrench functions, the sufficiency metric ϵ_S for $\vec{t} = \vec{0}$, and the attractors for the square (a) based on the exact model and (b) based on the simplified model (see text).

grasp solution. The other minima are generated at contact locations where the local wrench gradient, G, is orthogonal to the residual vector, $\vec{\rho}$.

Force Closure Behavior

The force closure behavior is based on a smoothed force domain model of the object. One such "smooth" approximation is the projection of the force domain model of the object onto sinusoidal basis functions with characteristic frequency of $1\frac{cycle}{2\pi\ rad}$. The force and moment diagrams projected onto the 1^{st} harmonic basis yields:

$$
\begin{aligned}
w_1 &= f_x = -cos(\theta)cos(\phi) & \quad w_4 &= m_x = 0 \\
w_2 &= f_y = -sin(\theta)cos(\phi) & \quad w_5 &= m_y = 0 \\
w_3 &= f_z = -sin(\phi) & \quad w_6 &= m_z = 0
\end{aligned}
$$

Note that using this approximation for n-fold symmetries reduces the control of grasp sufficiency (wrench closure) to a force closure optimization. This is due to the fact that the moment diagrams for n-fold symmetries exhibit characteristic frequencies of $n\frac{cycle}{2\pi}$ and are therefore ignored in the 1^{st} harmonic approximation. Moreover, it can be shown that this wrench model yields a convex sufficiency metric over a portion of the contact configuration space in the planar case when the task wrench bias $\vec{t} = \vec{0}$ (see [6]).

The sufficiency metric for this force closure model yields:

$$
\begin{aligned}
\epsilon_S^{FC} = & \left[t_{fx} + \frac{1}{n}\sum_{i=1}^{n} cos(\theta_i)cos(\phi_i) \right]^2 + \\
& \left[t_{fy} + \frac{1}{n}\sum_{i=1}^{n} sin(\theta_i)cos(\phi_i) \right]^2 + \\
& \left[t_{fz} + \frac{1}{n}\sum_{i=1}^{n} sin(\phi_i) \right]^2
\end{aligned}
\tag{4}
$$

The gradient of Equation 4 with respect to θ_k yields:

$$
\frac{\partial \epsilon_S^{FC}}{\partial \theta_k} = (A_{\theta k}^2 + B_{\theta k}^2)^{1/2} sin(\theta_k + \psi_k) \tag{5}
$$

where $A_{\theta k}$, $B_{\theta k}$, and ψ_k are constants independent of θk:

$$
\begin{aligned}
A_{\theta k} &= \frac{2}{n}\left(t_{fy} + \frac{1}{n}\sum_{i \neq k}(sin(\theta_i)cos(\phi_i)) \right) cos(\phi_k) \\
B_{\theta k} &= -\frac{2}{n}\left(t_{fx} + \frac{1}{n}\sum_{i \neq k}(cos(\theta_i)cos(\phi_i)) \right) cos(\phi_k) \\
\psi_k &= tan^{-1}(A_{\theta k}/B_{\theta k})
\end{aligned}
$$

This result demonstrates that the sufficiency metric employing the force closure model generates a unimodal error function. Figure 1(b) illustrates the wrench functions, $f_x(\theta)$, $f_y(\theta)$, *and* $m_z(\theta)$, the sufficiency metric, and the positions of attractors in the metric space for the smoothed sufficiency metric for the square shape.

In order to improve the controller's performance and in order to allow for composition with other convex controllers, we developed a convex version of the force closure controller, computing the force closure gradient over a quadratic with the same stable minima (a similar quadratic regulator for ϕ_k can be derived by differentiating Equation 4 with respect to ϕ_k – see [6]):

$$\left.\frac{\partial \epsilon_S}{\partial \theta}\right|_{\theta k}^{FC} = 2\frac{\epsilon_S^{FC} - \epsilon_S^*}{(\theta_k - \theta_k^*)} \tag{6}$$

where ϵ_S^* is the force closure error for $\theta_k = \theta_k^*$ and θ_k^* is the angle θ in which contact k minimizes ϵ_S^{FC}:

$$\theta_k^* = -tan^{-1}\left(\frac{A_{\theta k}}{B_{\theta k}}\right). \tag{7}$$

Moment Closure Behavior

The approximate wrench models employed in the force closure behavior generate predictable, unimodal control surfaces but disregards a great deal of information in order to do so. The solution generated in this fashion is, therefore, not always expected to be consistent with the minima in the *real* error surface (Figure 1). A local, moment closure optimization can be employed based on enriched force domain information.

Following convergence of the force closure behavior, contacts are positioned on particular planar facets of the object. The moment closure optimization will adjust the contact placement to eliminate any residual moment in the grasp. We use the perpendicular of a plane, (r_0, θ_0, ϕ_0), to parameterize the contact plane. Figure 2 illustrates the parameterization and the geometry from which the wrench models are derived. The forces transmitted through any planar face are constant at all contact positions on that face. The moments applied to the object, $\vec{m} = \vec{r} \times \vec{f}$, vary linearly with surface coordinate and pass through zero where the perpendicular passes through the plane. The resulting wrench model is:

$$\begin{aligned} w_1 &= f_x = -cos(\theta_0)cos(\phi_0) \\ w_2 &= f_y = -sin(\theta_0)cos(\phi_0) \\ w_3 &= f_z = -sin(\phi_0) \end{aligned}$$

$$w_4 = m_x = -r_\theta sin(\phi_0)cos(\theta_0) + r_\phi sin(\theta_0)$$

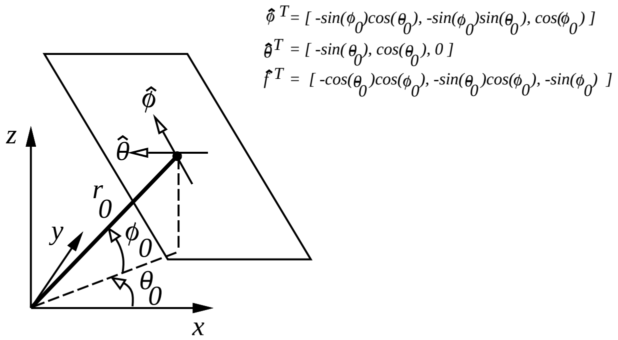

Figure 2: The Moment Closure Model derived from a Parametric Object Plane

$$\begin{aligned} w_5 &= m_y = -r_\theta sin(\phi_0)sin(\theta_0) - r_\phi cos(\theta_0) \\ w_6 &= m_z = r_\theta cos(\phi_0) \end{aligned} \tag{8}$$

where $(\hat{r_\theta}, \hat{r_\phi})$ are the surface coordinates of the contact in the plane. Note that this local planar surface approximation yields constant contact forces which implies that control is derived from the moment diagrams exclusively.

The moment closure sufficiency metric can be written as follows.

$$\begin{aligned} \epsilon_S^{MC} = & \left[t_{fx} - \frac{1}{n}\sum_i f_{xi}\right]^2 + \\ & \left[t_{fy} - \frac{1}{n}\sum_i f_{yi}\right]^2 + \\ & \left[t_{fz} - \frac{1}{n}\sum_i f_{zi}\right]^2 + \\ & \left[t_{mx} - \frac{1}{n}\sum_i m_{xi}\right]^2 + \\ & \left[t_{my} - \frac{1}{n}\sum_i m_{yi}\right]^2 + \\ & \left[t_{mz} - \frac{1}{n}\sum_i m_{zi}\right]^2 \end{aligned} \tag{9}$$

The convexity of the controller based on the gradient of ϵ_S^{MC} can be easily demonstrated if surface coordinates are used, but it doesn't necessarily hold if polar coordinates are used instead. We developed a convex version of the controller with polar coordinates using a quadratic regulator with the same equilibrium state as the original convex metric, similarly to the convex version of the force closure regulator. The planar surface coordinate where the gradient of ϵ_S^{MC} with respect to r_θ vanishes is given by

$$\begin{aligned} r^*_{\theta k} \;=\; & -\left[nt_{mx} - \sum_{i\neq k} m_{xi}\right](sin(\phi_0)cos(\theta_0))_k \\ & -\left[nt_{my} - \sum_{i\neq k} m_{yi}\right](sin(\phi_0)sin(\theta_0))_k \\ & +\left[nt_{mz} - \sum_{i\neq k} m_{zi}\right](cos(\phi_0))_k \end{aligned}$$

The corresponding θ coordinate of this minimum is:

$$\theta^*_k = tan^{-1}\left[\frac{r^*_{\theta k}}{r_0}\right] \tag{10}$$

so that,

$$\left.\frac{\partial \epsilon_S}{\partial \theta}\right|^{MC}_{\theta k} = 2\frac{\epsilon_S^{MC} - \epsilon_S^*}{(\theta_k - \theta^*_k)}. \tag{11}$$

A similar result for the moment closure regulator in the $\hat{\phi}$ direction can be derived by differentiating Equation 8 with respect to ϕ_k.

Behavior Composition

The goal of the grasp estimator is to generate a sufficient contact geometry. The problem is formulated as an optimization of the sufficiency metric, but this metric exhibits local minima which do not yield sufficient grasp configurations. This problem is addressed by employing two distinct control surfaces — the first (force closure) is based on coarse information and effectively circumvents local minima, the second (moment closure) is based on precise local information and can be used to refine the contact geometry locally. Composing force and moment closure behaviors can achieve a sufficient grasp geometry more frequently than using either behavior by itself.

Wrench Closure Composition

For a single linear decision surface, with an exponential switching profile, the activation A_i for behavior i is computed as

$$A_i = \frac{e^{\gamma_i}}{\sum_j e^{\gamma_j}} \tag{12}$$

where γ_i is a linear, parametric function of the error metric for contact i. Combinations of parameters can be used to adjust the position, orientation, and switch profile of the decision surface[6].

To compose the force and moment closure behavior, we used a single decision surface to distinguish two linearly separable activation domains in the error space — or equivalently a single radially symmetric activation function in the state space. This is a relatively inexpressive composition rule, but is sufficient for the class of objects presented in this paper. The activation of the wrench closure behaviors are:

$$A_{FC} = \frac{e^{(\gamma_{FC}-\gamma_{MC})}}{(1+e^{(\gamma_{FC}-\gamma_{MC})})} \tag{13}$$

$$A_{MC} = 1 - A_{FC} \tag{14}$$

If $d\epsilon_S^{FC}/d\vec{\psi}_k$ and $d\epsilon_S^{MC}/d\vec{\psi}_k$ are the gradients for force closure and moment closure respectively, where $\vec{\psi}_k = (\theta, \phi)_k$ is the coordinate of contact k, then the composite gradient is computed:

$$\frac{d\epsilon_S}{d\vec{\psi}_k} = A_{FC}\frac{d\epsilon_S^{FC}}{d\vec{\psi}_k} + A_{MC}\frac{d\epsilon_S^{MC}}{d\vec{\psi}_k}. \tag{15}$$

The controller employed to regulate wrench closure is derived from the composite gradient:

$$\Delta\vec{\psi}_k = -K_{WC}\frac{d\epsilon_S}{d\vec{\psi}_k} \tag{16}$$

Figure 3 is a plot of the behavior activation profile for one of two fingers during grasp formation on the square shape. These results are qualitatively the same as for all numbers of contacts and over all shapes that we evaluated. The grasp synthesis process can be viewed as a force closure heuristic directing a "best only" search which is subsequently optimized locally. The proposed composition of convex controllers generates a number of distinct solutions. In fact, the value of the equilibrium error can be used to identify topologically distinct solutions, each of which can be realized in an infinite number of geometric solutions. These behaviors are capable of producing "correct" grasps for n-fold, convex, rotationally symmetric objects. This follows from the observation that if the force closure regulator is permitted to run until convergence, then the moment

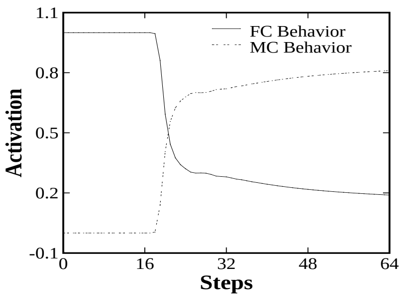

(a)

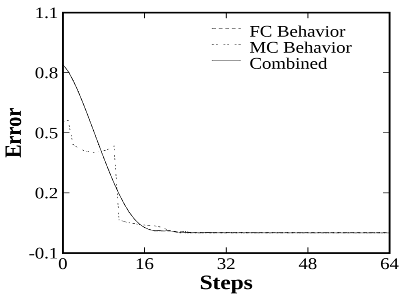

(b)

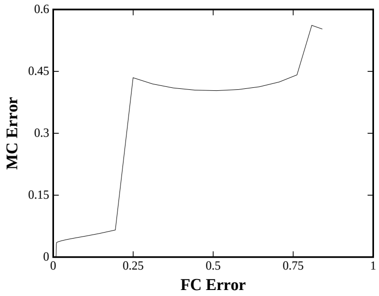

(c)

Figure 3: Wrench closure control dynamics for the formation of a grasp: (a) activation profile, (b) force and moment closure sufficiency error, and (c) the resulting trajectory in the wrench closure error plane.

closure behavior does not need to leave the current object face to eliminate any residual moment.

The performance of the system was evaluated on the planar shapes illustrated in Figure 4. Two, three or four contacts were placed at random initial locations on each shape, and the wrench controller ran until convergence. For each number of contacts and each shape, a total of 100 trials were performed. Figure 4 also illustrates all the distinct grasps that were generated by the controller for the test shapes.

Figure 5 shows the distribution of run-time required for convergence of the grasping behaviors for this sample.

Table 1 reports the mean number of single control steps until convergence from random initial configurations, as well as its standard deviation. Typically, the average number of steps until convergence for all shapes stayed in the range from 40 to 120 control steps. [1] A single step in the controller is one adjustment of the contact configuration, that is, a single adjustment of all n contacts. The algorithm is $O(n^2)$ each step, where n is the number of contacts. For a 4 contact grasp estimator, this corresponds to 1.8 milliseconds of CPU time per step on SPARCstation 2 workstation. This complexity can be reduced for large n by running n-$O(n)$ controllers — one for each contact position.

[1] The number of control steps is greatly determined by the gains selected. The gains used to generate Table 1 were *detuned* slightly to match rates with other behaviors not reported in this paper. Higher gains can be used for stand-alone grasp synthesis. In this case, one quarter of the steps reported in Table 1 were typical.

Conclusion

The approach described in this paper is designed to achieve some degree of local competence in multifingered robot hands executing dextrous grasps. The goal is to react to sensor data acquired during the execution of a grasp and in so doing, avoid expensive a priori models and detailed grasp plans. We demonstrated the grasp estimators performance on convex polygons; however, no extensions are required to handle general convex shapes and we have in fact already used the estimator in this fashion. The results support the value of this approach for improving the run-time performance of controllers for high dimensional systems. The proposed controller was examined while it performed grasp estimates from random initial configurations, rather than from planned contact configurations. The result for this class of objects suggests that the estimator can succeed in optimizing the grasp from arbitrarily bad initial grasp geometries, and could, in fact, alleviate the need for planning grasps at all for this class of objects.

We also devised a means for extracting object models from vision and proprioceptive information in the hand. This sensory apparatus permits an object model to be constructed incrementally during grasp formation. It is possible that the same model can provide a reactive context for reflexive behavior composition. We view this currently as a reinforcement learning problem where knowledge about object geometry influences the composition of reflexive grasp estimators. The choice of the behaviors presented in this paper was heavily influenced by a commitment to incremental, sensor-based reactive controllers and

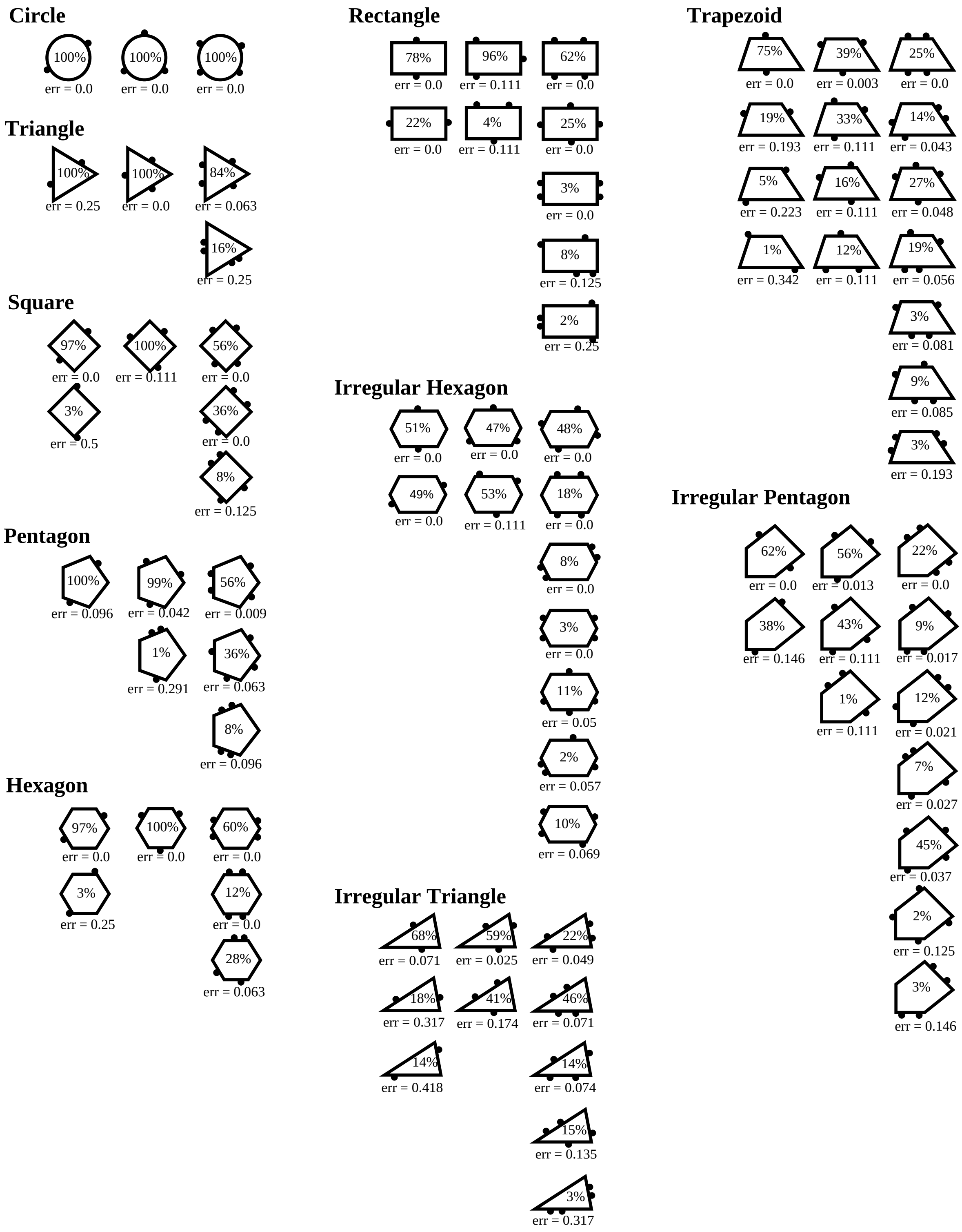

Figure 4: The grasp types for all objects tested. Percentages reported represent the fraction of random initial contact configurations that led to each solution type. Also recorded is the residual wrench closure error at convergence.

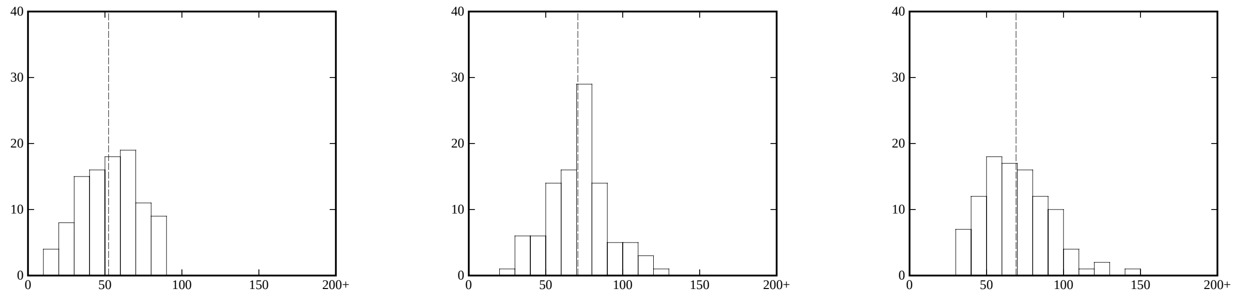

(a) 2 contacts (b) 3 contacts (c) 4 contacts

Figure 5: Histogram of number of steps until convergence for 2, 3, and 4 contacts for the pentagon.

Object	Cont.	Avg Steps	Stand. Dev.	Object	Cont.	Avg Steps	Stand. Dev.
Circle	2	39.45	10.78	Trapezoid	2	78.91	45.36
	3	59.02	14.17		3	89.72	36.51
	4	60.07	16.91		4	70.61	30.68
Triangle	2	58.74	15.18	Irregular Triangle	2	73.91	35.86
	3	124.78	62.85		3	94.08	41.89
	4	67.65	23.92		4	86.15	39.13
Square	2	60.46	20.20	Rectangle	2	62.50	19.28
	3	69.61	19.22		3	76.96	28.19
	4	71.25	20.85		4	74.12	20.63
Pentagon	2	52.37	18.32	Irregular Pentagon	2	66.59	23.04
	3	70.86	20.05		3	71.23	19.77
	4	69.19	21.73		4	80.24	31.22
Hexagon	2	56.97	18.36	Irregular Hexagon	2	57.48	20.92
	3	88.88	28.33		3	69.18	22.99
	4	69.23	15.54		4	67.00	19.61

Table 1: Numbers of steps until convergence, averaged over 100 trials.

to the learning problem.

References

[1] R.A. Brooks. A robust layered control system for a mobile robot. *IEEE J. Robotic Automat.*, 2(1):14–23, Mar. 1986.

[2] R.A. Brooks. Intelligence without representation. In *Proc. Workshop on the Foundations of AI.* The MIT Press, 1987.

[3] M.R. Cutkosky. On grasp choice, grasp models, and the design of hands for manufacturing tasks. *IEEE Trans. Robotics Automat.*, 5(3), June 1989.

[4] B. Faverjon and J. Ponce. On computing two-finger force-closure graps of curved 2d objects. In *Proc. 1991 IEEE Int. Conf. Robotics Automat.*, volume 1, pages 424–429, Sacramento, CA, May 1991.

[5] R.A. Grupen, K. Biggers, T.C. Henderson, and S. Meek. Task defined internal grasp wrenches. Technical Report UUCS-88-001, Department of Computer Science, University of Utah, 1988.

[6] R.A. Grupen, J.A. Coelho Jr., and K.X. Souccar. On-line grasp estimator: A partioned state space approach. Technical Report COINS Technical Report 92-75, COINS Department, University of Massachusetts, Oct. 1992.

[7] J.W. Jameson and L.J. Leifer. Automatic grasping: An optimization approach. *IEEE Trans. Syst., Man, Cybern.*, SMC-17(5), Sept./Oct. 1987.

[8] J. Kerr and B. Roth. Analysis of multifingered hands. *Journal of Robotics Research*, 4(4):3–17, Winter 1986.

[9] M.T. Mason and J. Kenneth Salisbury, editors. *Robot Hands and the Mechanics of Manipulation.* The MIT Press, Cambridge, MA, 1985.

[10] Y. Nakamura and H. Hanafusa. Optimal redundancy control of robot manipulators. *The Int. J. Robotics Res.*, 6(1), 1987.

[11] V.D. Nguyen. Constructing stable grasps. *The Int. J. Robotics Res.*, 8(1):26–37, 1989.

[12] M.H. Raibert. *Legged Robots that Balance.* The MIT Press, Cambridge, MA, 1986.

[13] J. Kenneth Salisbury. *Kinematic and Force Analysis of Articulated Hands.* PhD thesis, Stanford University, Stanford, CA, May 1982.